

Antireflection Coatings Combining Silicon Nitride with Silicon Nanoparticles

M. Beye¹, F. Ndiaye², and A. S. Maiga²

¹ *Department of Applied Physics, Gaston Berger University of Saint Louis, Senegal.*

² *Laboratory of Electronics, Data Processing, Telecommunications and Renewable Energies, Saint Louis, BP 234, Senegal*

Abstract—In this work, solar cell antireflection coatings (ARC) combining silicon nitride layer with silicon nanoparticles are investigated. Two configurations are considered: silicon nanoparticles on a SiN_x layer surface and partially embedded in a SiN_x layer. Numerical results show that this ARC concept performs better in the configuration where silicon nanoparticles are placed on the dielectric layer. A silicon nitride refractive index of 2.3 is found to be more advantageous, yielding a low weighted reflectance of 2.1% in the wavelength range 300 – 1100 nm. The stability of the reflectance for oblique incidence with angles lower than 40° was also observed. With this new ARC concept, a relative increase of 8.6% in the short circuit current density over a solar cell with the standard Si₃N₄ coating can be expected.

Index Terms—Silicon nitride, silicon nanoparticles, antireflection coatings

I INTRODUCTION

Silicon nitride (SiN_x) layers are largely used in photovoltaic (PV) applications due to their interesting optical and electrical properties [1]. Planar layers of this and other dielectric materials, generally used as antireflection coatings (ARCs) in solar cells and other optoelectronic devices, are often optimized for a single wavelength. Therefore, they reduce the reflection from a surface in a narrow wavelength range. It has been shown that an optimized SiN_x double layer has a little advantage over the standard Si₃N₄ single layer [2, 3].

Scattering from metal particles has been demonstrated to efficiently couple light into waveguide modes in thin semiconductor layers due to their surface plasmon resonances [4, 5]. Metal and dielectric nanoparticles have been also largely used to enhance light absorption in thin film solar cells [6 - 12]. Metal nanoparticles embedded in a dielectric layer [13, 14] and patterned on it or directly onto a substrate [15, 16] have been found to reduce the reflection from a solar cell active layer surface over a broad spectral range. Recently, a new approach not involving metals has been proposed, in which a two-dimensional periodic array of cylindrical silicon nanoparticles on a Si₃N₄ spacer layer is used. Simulations and experimental results showed a weighted reflectance lower than 2% over the spectral range 450 – 900 nm for angles of incidence up to ± 60° [17].

In this work, we consider a solar cell antireflection coatings combining silicon nitride layer with silicon nanoparticles in two configurations: silicon nanoparticles on a SiN_x layer surface and partially embedded in a SiN_x layer. The effect of the dielectric layer refractive index and the one related to the incorporation of silicon nanoparticles in the dielectric layer on the performances of this ARC concept are investigated.

II MODELS DESCRIPTION AND OPTIMIZATION PROCEDURE

We consider a silicon solar cell surface of length L and width l , on which a regular array of spherical silicon

nanoparticles is arranged as schematically shown in Fig. 1. In this figure r is the radius of a particle and p the period of the two-dimensional array.

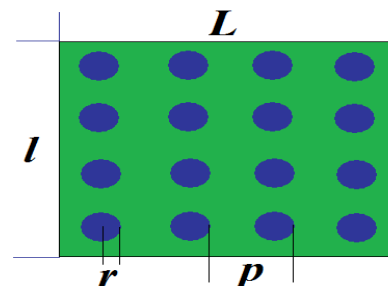


Figure 1: Schematic representation of a regular array of spherical silicon nanoparticles.

The two configurations considered in this work are shown in Fig. 2.

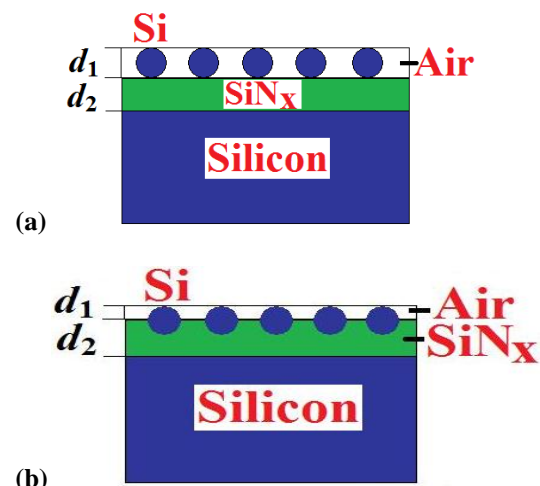


Figure 2: Schematic representations of ARCs:

(a) Silicon nanoparticles on a SiN_x layer surface;

(b) Silicon nanoparticles embedded in a SiN_x layer.

For each configuration, a modified transfer matrix method [18, 19, 20] is used to calculate the reflectance from the silicon surface. The ARC structures represented in Fig. 2 can be considered as composed of two layers (therefore, three interfaces) on a Si substrate (Fig. 3). The amplitude of the uniform electrical field, \mathbf{E} , at any position in a layer, can be divided into two components: the transmitted, \mathbf{E}^+ , and the reflected component, \mathbf{E}^- .

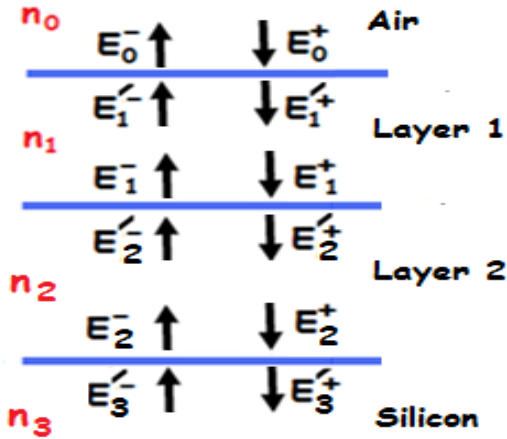


Figure 3: Notation of electric field amplitudes in the two-layer ARC structure. The prime is used for waves at the down side of an interface.

The field amplitudes at the top and bottom side of an interface are related by the so-called transmission or refraction matrix of the interface, $I_{k-1,k}$, as follows [19]:

$$\begin{pmatrix} E_{k-1}^+ \\ E_{k-1}^- \end{pmatrix} = I_{k-1,k} \begin{pmatrix} E_k^+ \\ E_k^- \end{pmatrix} \quad (1)$$

where

$$I_{k-1,k} = \frac{1}{t_{k-1,k}} \begin{bmatrix} 1 & r_{k-1,k} \\ r_{k-1,k} & 1 \end{bmatrix} \quad (2)$$

The Fresnel coefficients of transmission, $t_{k-1,k}$, and reflection of the interface, $r_{k-1,k}$, are defined as follows [20]:

✓ For the s polarization:

$$t_{k-1,k} = \frac{2n_{k-1}q_{k-1}}{n_{k-1}q_{k-1} + n_k q_k} \quad (3)$$

$$r_{k-1,k} = \frac{n_{k-1}q_{k-1} - n_k q_k}{n_{k-1}q_{k-1} + n_k q_k} \quad (4)$$

✓ For the p polarization :

$$t_{k-1,k} = \frac{2n_k q_{k-1}}{n_k q_{k-1} + n_{k-1} q_k} \quad (5)$$

$$r_{k-1,k} = \frac{n_k q_{k-1} - n_{k-1} q_k}{n_k q_{k-1} + n_{k-1} q_k} \quad (6)$$

where n_k is the complex refractive index of the k -th layer and

$$q_k = \sqrt{1 - \left(\frac{n_0 \sin \theta_0}{n_k} \right)^2} \quad (7)$$

θ_0 is the angle of incidence.

The field amplitudes at the top and bottom side of the k -th layer are related by the so-called propagation matrix of the layer, P_k , as follows [18]:

$$\begin{pmatrix} E_k^+ \\ E_k^- \end{pmatrix} = P_k \begin{pmatrix} E_k^+ \\ E_k^- \end{pmatrix} \quad (8)$$

where

$$P_k = \begin{bmatrix} \exp(i\delta_k) & 0 \\ 0 & \exp(-i\delta_k) \end{bmatrix} \quad (9)$$

The phase shift, δ_k , due to the wave passing through the k -th layer is given by:

$$\delta_k = \left(\frac{2\pi}{\lambda} \right) n_k d_k \cos(\theta_k) \quad (10)$$

where λ is the wavelength of the incident light, n_k is again the complex refractive index of the k -th layer, d_k its thickness, and θ_k is the propagation angle following Snell's law ($n_0 \sin \theta_0 = n_1 \sin \theta_1 = n_2 \sin \theta_2 = n_3 \sin \theta_3$).

The above matrix transformations can be applied for the 2 layers and 3 interfaces in Fig. 3, resulting in:

$$\begin{pmatrix} E_0^+ \\ E_0^- \end{pmatrix} = I_{01} P_1 I_{12} P_2 I_{23} \begin{pmatrix} E_3^+ \\ E_3^- \end{pmatrix} \quad (11)$$

$$= \begin{bmatrix} T_{11} & T_{12} \\ T_{21} & T_{22} \end{bmatrix} \begin{pmatrix} E_3^+ \\ E_3^- \end{pmatrix}$$

The product matrix resulting from the above procedure is a 2×2 matrix called system transfer matrix T .

The complex reflection coefficient of the multilayer can be calculated from the elements of the system transfer matrix as follows [18, 19]:

$$r = \frac{E_0^-}{E_0^+} \Bigg|_{E_3^- = 0} = \frac{T_{21}}{T_{11}} \quad (12)$$

from which the reflectance, R , is obtained as $|r|^2$.

It is clear that to calculate R , we need to know the complex refractive index of each layer and its thickness. For the ARC configuration shown in Fig 2.a, the first layer can be considered as a composite material consisting of silicon nanoparticles in air (we suppose that $n_{\text{air}} = n_0 \approx 1$) with a thickness d_1 equal to the diameter of the nanoparticles and the second is a homogeneous SiN_x spacer layer of thickness d_2 . For the configuration shown in Fig. 2b, two layers of composite materials can be considered with the host media consisting of air and SiN_x , respectively. The complex refractive index of a material is related to its permittivity by the well-known formula: $\varepsilon = n^2$. Therefore, knowing the permittivity, we can calculate the complex refractive index.

The Maxwell-Garnett effective medium approximation is used to calculate the effective permittivity of the composite

materials formed by silicon nanoparticles in air and in SiN_x. This effective permittivity is given by [21]:

$$\epsilon_{eff} = \epsilon_b \frac{\epsilon_i(1+2f) + 2\epsilon_b(1-f)}{\epsilon_i(1-f) + \epsilon_b(2+f)} \quad (13)$$

where ϵ_b is the permittivity of the host (base) material, ϵ_i the permittivity of the particle's materials and f the volume fraction of the particles in the host medium.

For a layer of thickness d , its volume can be expressed as: $V_{layer} = L \times l \times d$. For simplicity, we will take $L = l = 1$ cm. The volume of a spherical particle of radius r is: $V_p = 4\pi r^3/3$. The number of particles on the surface can be expressed as: $N_p = (L/p) \times (l/p)$. Thus, the volume fraction of the particles in the corresponding layer is: $f = (N_p \times V_p) / V_{layer}$.

Optical data for silicon are taken from [22]. For silicon nitride, optical constants are calculated using data provided in the appendix of [23].

The reflectance weighted over the AM1.5G solar spectrum (Air Mass 1.5 Global: terrestrial solar spectral irradiance on a surface of specified orientation under specified atmospheric conditions) is evaluated in the wavelength range 300 – 1100 nm to take into account the influence of the photon flux and the solar cell internal quantum efficiency. This parameter is defined as [24]:

$$R_w = \frac{\int_{\lambda_{min}}^{\lambda_{max}} F(\lambda) \cdot IQE(\lambda) \cdot R(\lambda) \cdot d\lambda}{\int_{\lambda_{min}}^{\lambda_{max}} F(\lambda) \cdot IQE(\lambda) \cdot d\lambda} \quad (14)$$

where F is the photon flux, IQE the solar cell internal quantum efficiency, defined as the number of electrons collected per photon not reflected and R the reflectance.

The photon flux, F , is related to the irradiance, I , by the following expression [25]:

$$F(\lambda) = \frac{I \cdot \lambda}{h \cdot c} \quad (15)$$

where λ is the wavelength of the incident light, h the Planck's constant and c the speed of light. Irradiance data are taken from [26].

The short circuit current density (J_{sc}) is also evaluated as an important solar cells parameter. For a single junction solar cell, it is given by [23]:

$$J_{sc} = q \int_{\lambda_{min}}^{\lambda_{max}} F(\lambda) \cdot IQE(\lambda) \cdot A(\lambda) d\lambda \quad (16)$$

where $A(\lambda)$ is the absorption by silicon.

We suppose in this work that $IQE = 1$, meaning that all not reflected photons are collected. Thus, in equation (4), $A(\lambda)$ can be replaced by $[1 - R(\lambda)]$.

III SILICON NANOPARTICLES ON A SiN_x LAYER SURFACE

The weighted reflectance under normal incidence from the silicon surface in the configuration shown in Fig 2.a is about 17.3% for an array of spherical particles of diameter 125 nm, spaced by 450 nm and a Si₃N₄ layer thickness of 60 nm with a refractive index of 2.0. These values are the optimal ones found in [15] for cylindrical nanoparticles. This high reflectivity suggests that the dimensional parameters have to be re-optimized since the shape of the particles has changed.

The dependences of the weighted reflectance (R_w) on the period (p) of the regular array and the spacer layer thickness (d_2) are shown in Fig. 4. The parameters used in the calculations are displayed in Table I. It can be seen that there is an optimum both in the period and in the thickness. It is clear from the insets of Fig. 4a-b that these optimal values are about 840 nm for the period and 66 nm for the spacer layer thickness. It has been argued that the optimum in the array period is related to the fact that a smaller period results in a strong interparticle coupling effect and a large period corresponds to a small surface coverage, reducing the overall light scattering. The optimum in the spacer layer thickness is because thicker spacer layers lead to reduce the near field-coupling, while thinner layers cause a shift of the Plasmon resonance [16].

TABLE 1
Parameters used in the calculations.

Parameters	For Fig. 4a	For Fig. 4b
Diameter of particles (d_1)	125 nm	125 nm
Period (p)	variable	840 nm
Spacer layer thickness (d_2)	60 nm	variable

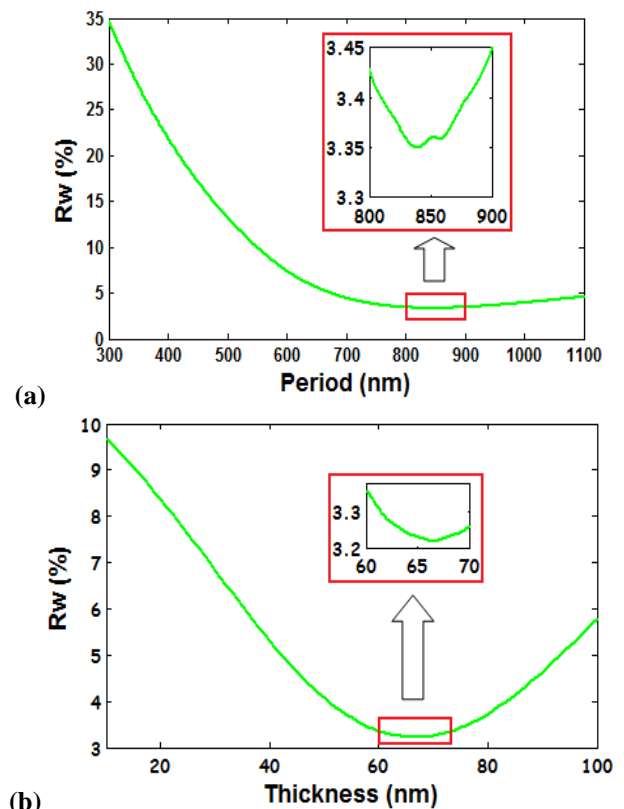


Figure 4: Dependences of the weighted reflectance on the dimensional parameters for a particle diameter of 125 nm:
(a) Period dependence of R_w ;
(b) Thickness dependence of R_w .

and coated with a standard 80 nm thick Si_3N_4 are also shown for comparison. The optimization of the dimensional parameters, except the particle's diameter, results in a decrease of the weighted reflectance from 17.3% to 3.2%.

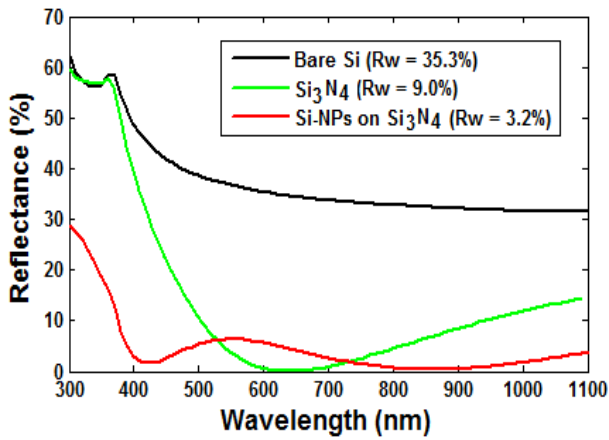


Figure 5: Reflectance under normal incidence from a bare silicon surface (black), a silicon surface coated with a 80 nm thick Si_3N_4 layer (green) and with a 60 nm thick SiN_x layer on which silicon nanoparticles of diameter 125 nm and spaced by 450 nm are arranged (red).

The strong reduction of the reflection is explained by the combined effect of the preferential forward scattering of the incident light by the silicon nanoparticles and the destructive interference from the SiN_x layer [17].

The scattering from particles is known to depend strongly on the dielectric environment. Figure 6 represents the dependence of the weighted reflectance on the SiN_x refractive index. For the optimal dimensional parameters found in Fig. 4, it appears that an optimal refractive index of about 2.3 leads to a weighted reflectance of 2.1%. However, it is well known that the extinction coefficient and, the absorption within a SiN_x layer, slightly increases in the lower wavelength range for high refractive indices [23]. Therefore, the pronounced antireflection effect for higher index may be partly compensated by the increased absorption within the layer. This claim may be verified by taking into account the dispersion of SiN_x optical constants.

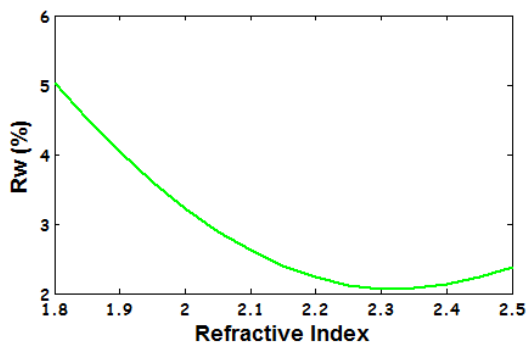


Figure 6: Dependence of R_w on the SiN_x refractive index for optimal dimensional parameters (diameter 125 nm, period 840 nm and spacer layer thickness 66 nm).

A good antireflection coating must be stable in a wide range of angles of incidence. Figure 7 shows the angular dependence of the weighted reflectance for the configuration shown in

Fig. 2a with the optimal parameters. It appears that the reflectance shows a good stability for angles of incidence under 40° .

An evaluation of the short circuit current density from equation (16) shows that for a solar cell with the standard Si_3N_4 single layer ARC, a theoretical J_{SC} value of 38.4 mA/cm^2 can be expected, whereas, for this new ARC concept with the optimal parameters this value is 41.7 mA/cm^2 , corresponding to a relative increase of about 8.6%.

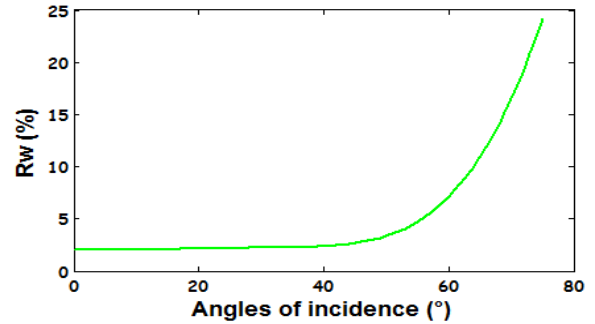


Figure 7: Angular dependence of the WR for the ARC configuration with optimal parameters.

IV SILICON NANOPARTICLES PARTIALLY EMBEDDED IN A SiN_x LAYER

For the configuration of silicon nanoparticles on a SiN_x layer with the optimal parameters (diameter 125 nm, period 840 nm, spacer layer thickness 66 nm, refractive index 2.3) let's incorporate gradually the nanoparticles in the dielectric layer. We can define a factor, F_{emb} , corresponding to the portion of a particle embedded in the SiN_x layer. Here, the maximum value of F_{emb} is $66/125$ or about 0.52, representing the ratio of the optimal spacer layer thickness over the optimal diameter of nanoparticles. The increase of the weighted reflectance with the factor F_{emb} (Fig. 8) permit to conclude that the embedded silicon nanoparticles in the SiN_x layer yield a negative effect. Therefore, the proposed ARC performs better in the configuration where silicon nanoparticles are placed on the SiN_x layer.

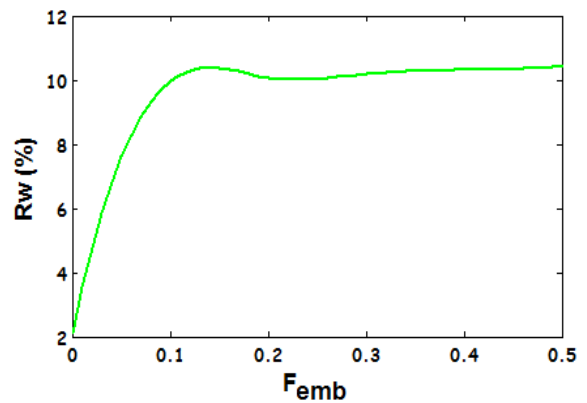


Figure 8: Dependence of R_w on the parameter F_{emb} under normal incidence for the ARC with optimal parameters.

V CONCLUSION

Two configurations of antireflection coating combining silicon nanoparticles and silicon nitride layer are considered. The antireflection performances of this combination are found to be better in the configuration where silicon nanoparticles are placed on the SiN_x layer. For this configuration, a SiN_x refractive index of 2.3 provides better performances, yielding a low weighted reflectance of 2.1% in the wavelength range 300 – 1100 nm. Stability of the reflectance for oblique incidence with angles lower than 40° is observed. A relative increase of 8.6% in the short circuit current density over a silicon solar cell with the standard Si₃N₄ coating can be theoretically expected. Partially embedded silicon nanoparticles in the dielectric layer yielded a negative effect. The new ARC concept proposed in this work can be used for efficiency improvement in silicon solar cells.

ACKNOWLEDGMENTS

The authors would like to thank the staff members of the Department of Applied Physics: A. Ndiaye, D. Diouf and M. Sene for helpful discussions and suggestions. This work was also supported by the University Gaston Berger (Grant N° 0003765).

REFERENCES

- [1] M. Lipiński, "Silicon nitride for photovoltaic application", *Archives of Materials Science and Engineering* **46**, 2 (2010) 69–87.
- [2] D. Gong, Y-J Lee, M. Ju, J. Ko, D. Yang, Y. Lee, G. Choi, S Kim, J. Yoo, B. Choi, and J. Yi, "SiN_x Double Layer Antireflection Coating by Plasma-Enhanced Chemical Vapor Deposition for Single Crystalline Silicon Solar Cells", *Japanese Journal of Applied Physics* **50**, 08KE01 (2011) 1–5.
- [3] Y. Lee, D. Gong, N. Balaji, Y. Lee, and J. Yi, "Stability of SiN_x/SiN_x double stack antireflection coating for single crystalline silicon solar cells", *Nanoscale Research Letters* **7**, 50 (2012) 1 – 6.
- [4] H. R. Stuart and D. G. Hall, "Island-size effects in nanoparticles-enhanced photodetectors", *Applied Physics Letters* **73**, 26 (1998) 3815–3817.
- [5] H. R. Stuart and D. G. Hall, "Absorption enhancement in silicon-on-insulator waveguides using metal island films", *Applied Physics Letters* **69**, 16 (1996) 2327–2329.
- [6] P. Matheu S. H. Lim, D. Derkacs, C. Mcpheeters, and E. T. Yu, "Metal and Dielectric Nanoparticle Scattering for Improved Optical Absorption in Photovoltaic Devices", *Applied Physics Letters* **93**, 191113 (2008) 1–3.
- [7] E. T. Yu, D. Derkacs, S. H. Lim, P. Matheu, and D. M. Schaadt, "Plasmonic Nanoparticle Scattering for Enhanced Performance of Photovoltaic and Photodetector Devices", *Proc. of SPIE* **7033** (2008) 70331V-1–70331V-9.
- [8] K. R. Catchpole and A. Polman, "Design Principles for Particle Plasmon Enhanced Solar Cells", *Applied Physics Letters* **93**, 191113 (2008) 1–3.
- [9] K. R. Catchpole, A. Polman, "Plasmonic solar cells", *Optics Express* **16**, 26 (2008) 21793–21800.
- [10] F. J. Beck, S. Mokkaṭpati, A. Polman and K. R. Catchpole, "Light Trapping For Solar Cells Using Localised Surface Plasmons in Self-Assembled Ag Nanoparticles", **24th** European Photovoltaic Solar Energy Conference, Hamburg, Germany (2009) 232–235.
- [11] K. C. Sahoo, M. K. Lin, E. Y. Chang, Y. Y. Lu, C. C. Chen, J. H. Huang, and C. W. Chang, "Fabrication of Antireflective Sub-Wavelength Structures on Silicon Nitride Using Nano Cluster Mask for Solar Cell Application", *Nanoscale Research Letters* **4** (2009) 680–683.
- [12] H. A. Atwater and A Polman, "Plasmonics for improved photovoltaic devices", *Nature Materials* **9** (2010) 205 – 213.
- [13] Y. Wang, N. Chen, X. Zhang, X. Yang, Y. Bai, M. Cui, Y. Wang, X. Chen and T. Huang, "Ag Surface Plasmon Enhanced Double-Layer Antireflection Coatings for GaAs Solar Cells", *Journal of Semiconductors* **30**, 7 (2009) 072005-1 – 072005-5.
- [14] R. Sircar, D. P. Srivastava and B. Tripathi, "Study of Ag Nanoparticle Embedded Silicon Nitride Anti-Reflection Coating (ARC) for Silicon Solar Cells", *International Journal of Photonics* **2**, 1 (2010) 7-14.
- [15] P. Spinelli, M. Hebbink, R. De Waele, L. Black, F. Lenzmann, and A. Polman, "Optical Impedance Matching using Coupled Plasmonic Nanoparticle Arrays", *Nano Letters* **11** (2011) 1760–1765.
- [16] P. Spinelli, V. E. Ferry, J. Van De Groep, M. Van Lare, M. A. Verschuuren, R. E. I. Schropp, H. A. Atwater, and A. Polman, "Plasmonic Light Trapping in Thin-Film Si Solar Cells", *Journal of Optics* **14** (2012) 1–11.
- [17] P. Spinelli, M. A. Verschuuren, and A. Polman, "Broadband Omnidirectional Antireflection Coating Based on Subwavelength Surface Mie Resonators", *Nature Communications* **3**, 692 (2012) 1–5.
- [18] C. C. Katsidis, and D. I. Siapkas, "General transfer-matrix method for optical multilayer systems with coherent, partially coherent, and incoherent interference", *Applied Optics* **41**, 19 (2002) 3978–3987.
- [19] M. C. Tropicovsky, A. S. Sabau, A. R. Lupini, and Z. Zhang, "Transfer-matrix formalism for the calculation of optical response in multilayer systems: from coherent to incoherent interference", *Optics Express* **18**, 24 (2010) 24715–24721.
- [20] S. A. Dyakov, V. A. Tolmachev, E. V. Astrova, S. G. Tikhodeev, V. Yu. Timoshenko, T. S. Perova, "Numerical methods for calculation of optical properties of layered structures", *Proc. of SPIE* Vol. **7521** (2010) 75210G-1–75210G-10.
- [21] R. Ruppini, "Evaluation of extended Maxwell-Garnett theories", *Optics Communications* **182** (2000) 273–279.
- [22] M. A. Green and M. Keevers, "Optical properties of intrinsic silicon at 300 K ", *Progress in Photovoltaics* **3**, 3 (1995) 189–192.
- [23] H. Nagel, A. G. Aberle, and R. Hezel, "Optimized Antireflection Coatings for Planar Silicon Solar Cells using Remote PECVD Silicon Nitride and Porous Silicon Dioxide", *Progress in Photovoltaics* **7** (1999) 245–260.
- [24] D. Bouhafs, A. Moussi, A. Chikouche, and J. M. Ruiz, "Design and simulation of antireflection coating systems

for optoelectronic devices: Applications to silicon solar cells”, *Solar Energy and Solar Cells* **52** (1998) 79–93.

- [25] S. A. Boden and D. M. Bagnall, “Sunrise to Sunset Optimization of Thin Film Antireflective Coatings for Encapsulated, Planar Silicon Solar Cells”, *Progress in Photovoltaics* **17** (2009) 241–252.
- [26] American Society for Testing and Materials (ASTM), “Standard Tables for Reference Solar Spectral Irradiance at air mass 1.5: ASTM G-173-03”, (2003).

M. Beye obtained his PhD in Applied Physics in 2013 from Gaston Berger University. He received his MS (2005) in Semiconductor Materials and Structures and BS (2003) degrees from the Saint-Petersburg Electrotechnical University (Russia). He held different teaching positions since 2006, particularly at the Department of Applied Physics of the Gaston Berger University which he joined in

2010. He has also worked at the Laboratory of Electronics, Data Processing, Telecommunications and Renewable Energies. His research interest includes antireflection coating technologies, solar cells and related topics, nanotechnology, environment.

F. Ndiaye is a PhD Student at the Laboratory of Electronics, Data Processing, Telecommunications and Renewable Energies of the Gaston Berger University. She is working on the relations between environmental conditions and PV module performances.

A. S. Maiga obtained his PhD in 1993 from the University of Rennes (France). He is now an Associate Professor at the Department of Applied Physics of the Gaston Berger University. He is also leading the Laboratory of Electronics, Data Processing, Telecommunications and Renewable Energies.